

# Variation of the dielectric constant of anodic oxide films on titanium with oxygen evolution

M. A. ABDEL RAHIM

*Department of Chemistry, Faculty of Science, University of Cairo, Giza, Egypt*

Received 5 May 1993; revised 16 January 1995

Titanium was anodized potentiodynamically in acidic solution of pH 3 ( $\text{Na}_2\text{SO}_4 + \text{H}_2\text{SO}_4$ ) in the potential region before and at oxygen evolution. The oxide film growth efficiency in the range of potential above oxygen evolution was investigated using galvanostatic charging curves. A value of 62% for the efficiency was estimated. The conductivity characteristics of the oxide film formed in the two regions were investigated on the basis of the variation of the dielectric constant. Values of 18.2 and 39.7 for the dielectric constant were obtained for oxides formed in the region before and at the oxygen evolution potential, respectively.

## 1. Introduction

Titanium behaves as a typical valve metal, but the anodic oxide film is electrochemically less stable than the barrier films formed on Al, Ta and Nb [1]. A homogeneous oxide film of  $\text{TiO}_2$  was proposed as being formed on titanium by anodic oxidation [1–3]. During titanium anodization, oxygen evolution is always observed, accompanied by a sudden decrease in the current efficiency for the film formation [4]. Under certain conditions, the oxide film was found to thicken rapidly simultaneously with oxygen evolution [1].

The physico-chemical properties of the  $\text{TiO}_2$  are influenced by the loading of the film by incorporated species [5]. Depending on the rate of oxide film formation, various dielectric constant values for  $\text{TiO}_2$  were obtained [6]. Values ranging from 30 to 68 were obtained for the dielectric constant of  $\text{TiO}_2$  [6–8]. The variation of the dielectric constant may change the conductivity characteristics of the titanium oxide films.

The work presented here reports on the variation of the dielectric constant of oxide films formed on titanium metal during anodization. A method is also presented for the estimation of the dielectric constant.

## 2. Experimental details

The electrochemical cell was described previously [9]. The titanium electrodes were in the form of rods (Koch light 99.9%) of apparent surface area  $0.984 \text{ cm}^2$  mounted on assemblies in which only glass and Teflon, besides the electrode, came in contact with the solution. The electrical contact was made by screwing a copper rod inside the titanium rod to a depth of about 3.0 mm. Another titanium electrode in the form of a disc ( $0.2 \text{ cm}^2$  area) was used for capacitance measurements.

AR chemicals were used as received without further

purification. Solutions were prepared from mixtures of  $0.5 \text{ M Na}_2\text{SO}_4 + 0.01 \text{ M H}_2\text{SO}_4$ ; these were of pH 3. The pH was checked using a precision pH meter.

Charging curves were measured using a 'Princeton' galvanostat. Potentiodynamic anodization was performed on titanium at a scan rate of  $1 \text{ mV s}^{-1}$  using a potentiostat and an XY recorder.

Oxide films were formed potentiodynamically on mechanically polished titanium electrodes in aerated  $\text{Na}_2\text{SO}_4/\text{H}_2\text{SO}_4$  (pH 3) solution. In another set of experiments the potentiodynamically formed oxides were further stabilized potentiostatically for about 4 h at constant potential; this potential corresponded to the film formation potential. Capacitance measurements at 1 kHz were used to estimate the dielectric constant of the oxide film. The alternating current bridge, used for the capacitance measurements, was a simple conventional bridge of the symmetrical Wein type, of which the known arm was a capacitor in series with a resistor. All potentials given here are referred to the  $\text{Hg}/\text{Hg}_2\text{SO}_4$  reference electrode.

## 3. Results and discussion

### 3.1. Anodic formation of oxide films on titanium

Using the linear potential sweep method, stoichiometric oxide films of uniform thickness were formed during the anodic oxidation of titanium in aqueous electrolyte solution [2]. There is strong evidence, that the oxide films are predominantly composed of  $\text{TiO}_2$  [1–3].

A potentiodynamic curve of a mechanically polished titanium in aerated  $\text{Na}_2\text{SO}_4 + \text{H}_2\text{SO}_4$  (pH 3) at a scan rate of  $1 \text{ mV s}^{-1}$  is shown in Fig. 1. This Figure shows: (i) the first passivation peak lies at a potential of  $-1.04 \text{ V}$ ; (ii) the second peak is at a potential of about  $-0.53 \text{ V}$ ; (iii) oxygen evolution starts at  $+1.5 \text{ V}$ . This is characterized by an increase

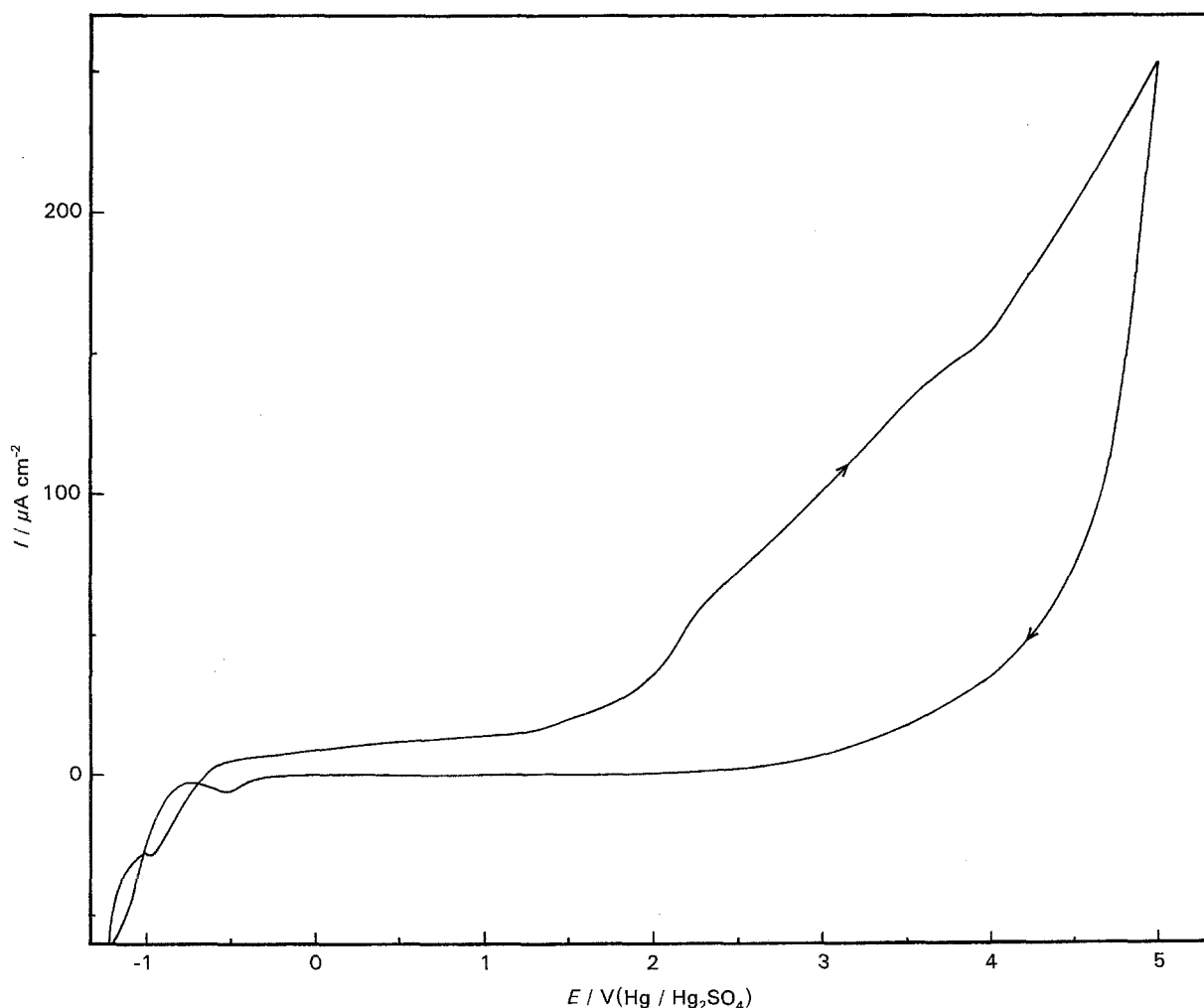


Fig. 1. Potentiodynamic polarization curve on titanium in aerated solution of  $\text{Na}_2\text{SO}_4 + \text{H}_2\text{SO}_4$  (pH 3).

in the current which continued up to +5.0 V; (iv) the reduction peak lies at  $-0.5$  V.

From these observations it may be concluded that a stable oxide layer is formed on titanium in the sulphate mixture (pH 3) in the range of potential extending from  $-1.04$  to  $+1.50$  V in the anodic direction and up to  $-0.5$  V in the cathodic direction.

### 3.2. Determination of the dielectric constant

A set of successive potentiodynamic curves at a single scan rate of  $10 \text{ mV s}^{-1}$  was carried out in the tested solution. The potential was scanned from  $-1.2$  V up to  $0.2$  V in the anodic direction and the scan was reversed in the cathodic direction to  $0$  V. At this potential, the polarization was switched off and the open-circuit capacitance of the formed oxide was measured immediately at a fixed frequency of  $1 \text{ kHz}$ . The procedure was repeated to a successively higher potential in the anodic direction, before reversing the scan and measuring the capacitance at  $0$  V. The values of the maximum voltage reached were  $0.4, 0.6, 0.8, 1.0, 1.5, 2.0, 2.5, 3.0$  and  $3.5$  V.

The area under the potentiodynamic curves was graphically estimated and used to determine the oxide film thickness at each formation potential using

the following relation [10]:

$$d = d_0 + \frac{M}{nF\delta_{\text{ox}}} \int_0^t i dt \quad (1)$$

where  $d$  is the oxide film thickness,  $d_0$  is initial film thickness (a value of  $1.0 \text{ nm}$  was used [6])  $\delta_{\text{ox}}$  is the film density,  $M$  is the molecular weight,  $n$  is the number of electrons exchanged and  $F = 96490 \text{ C mol}^{-1}$ . The quantity  $M/nF\delta_{\text{ox}}$  represents the volume of oxide formed per coulomb, a value of  $5.37 \times 10^{-5} \text{ cm}^3 \text{ C}^{-1}$  was used here [11].

To calculate the current efficiency, some galvanostatic charging curves (potential against time at constant current density) were performed on titanium in the test solution ( $\text{H}_2\text{SO}_4 + \text{Na}_2\text{SO}_4$ ; pH 3). The results are represented in Fig. 2 which shows a change of gradient in the charging curves in the potential range of oxygen evolution. For each charging curve in Fig. 2, the slope of the straight lines was determined below and above the change of gradient (oxygen evolution). This slope  $(dE/dt)_i$  can be taken as a measure of the oxide formation rate [12]. Assuming 100% efficiency for the oxide growth below oxygen evolution [13]. The efficiency above oxygen evolution can be calculated by comparing the slopes of the charging curves at each current density. A value of 62% was calculated for the efficiency of oxide growth

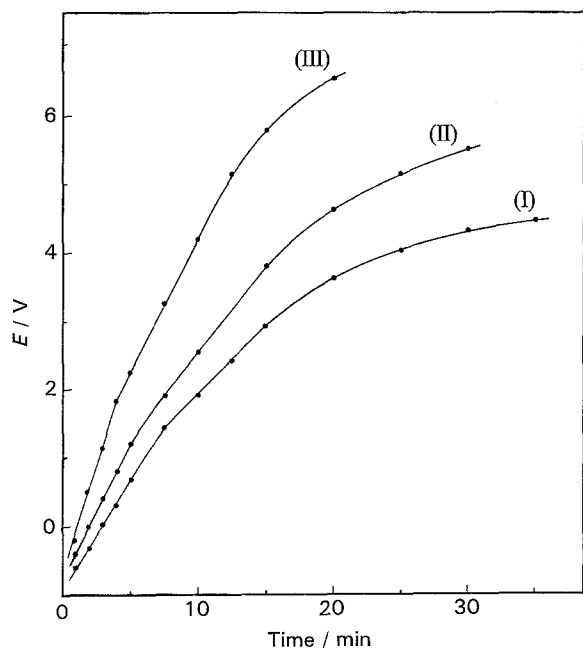


Fig. 2. Anodic charging curves on titanium in Na<sub>2</sub>SO<sub>4</sub>+H<sub>2</sub>SO<sub>4</sub> solution (pH 3) at (I) 20, (II) 30 and (III) 50 μA cm<sup>-2</sup>.

in the range of potential above the oxygen evolution region. This value of the current efficiency was used together with Equation 1 to calculate the oxide film thickness above the oxygen evolution potential (>1.5 V).

Table 1 represents the calculated film thickness, using Equation 1, at each formation potential. A plot of the film thickness against 1/C, where C is the measured capacitance, is shown in Fig. 3 which shows two straight lines, one at the potential range before the partial oxygen evolution (extending up to 1.0 V) and the other after this potential range (extending from 1.5 to 3.5 V). From the slope of the two straight lines, two values for the dielectric constant are obtained using

$$d = \frac{Da}{(4\pi C) \times 9 \times 10^9} \quad (2)$$

where C (F) is the capacitance, D is the dielectric constant and a (m<sup>2</sup>) is the electrode area. Values of 18.2 and 39.7 are obtained for the dielectric constant of the oxide formed below and above the oxygen evolution potential, respectively.

It must be emphasized that the estimation of the

Table 1. Charge consumed in the formation of the oxide film and the corresponding oxide thickness at different formation potentials

$E_f/V$	$\int idt/10^{-3} C cm^{-2}$	$d/nm$
0.4	1.703	1.91
0.6	2.155	2.16
0.8	2.967	2.59
1.0	3.547	2.90
1.5	5.888	4.16
2.0	8.607	5.62
2.5	12.242	7.57
3.0	14.680	8.88
3.5	18.301	10.83

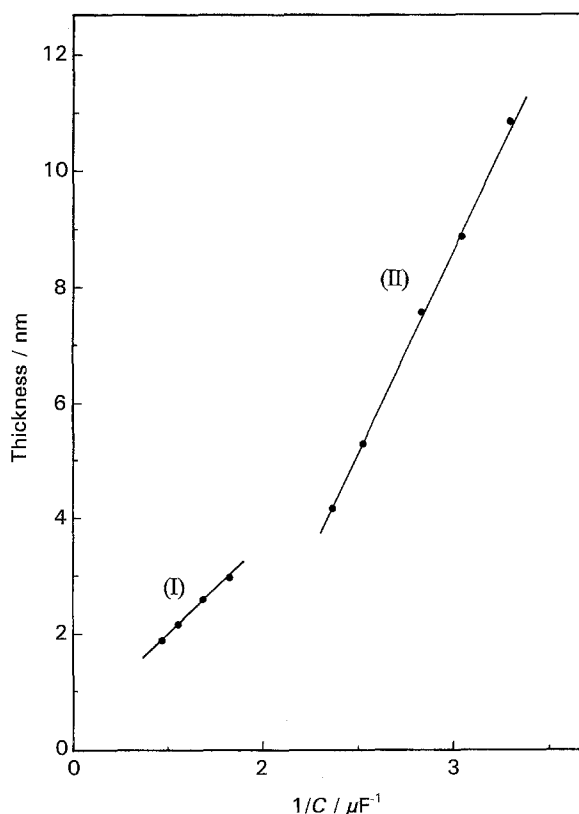


Fig. 3. Relation between the oxide thickness (calculated from coulometric measurements) and the reciprocal of capacitance. Oxides formed in the potential range (I) before and (II) within oxygen evolution.

film thickness from coulometric measurements is approximate. Two regions can be identified in Fig. 3. Region I represents the oxide formed in the region before oxygen evolution (as indicated by the potentiodynamic curve of Fig. 1). Region II represents the oxide formed in the region of potential at oxygen evolution. From the values determined for the dielectric constant, 18.2 and 39.7 in regions I and II, respectively, it is expected that the oxide formed in region I is more electrically conducting than that formed in region II. This is due to the low dielectric constant of the oxide (i.e., as the dielectric constant of the substance increases, it becomes more insulating). Similar values for the dielectric constant were reported elsewhere [6].

### 3.3. Estimation of the oxide film thickness

Oxide films of various thickness were obtained on titanium using the potentiodynamic method at a scan rate of 1 mV s<sup>-1</sup>. Different oxide thickness were obtained at different formation potentials. These formation potentials were chosen within the passive region at potentials of 0.2, 0.4, 0.6, 0.8 and 1.0 V before the oxygen evolution potential and 1.5, 2.0, 2.5, 3.0 and 3.5 V within the oxygen evolution potential region.

Capacitance measurements were used to calculate the oxide film thickness at each formation potential. The capacitance of the oxide was measured immediately at open-circuit potential after reaching the

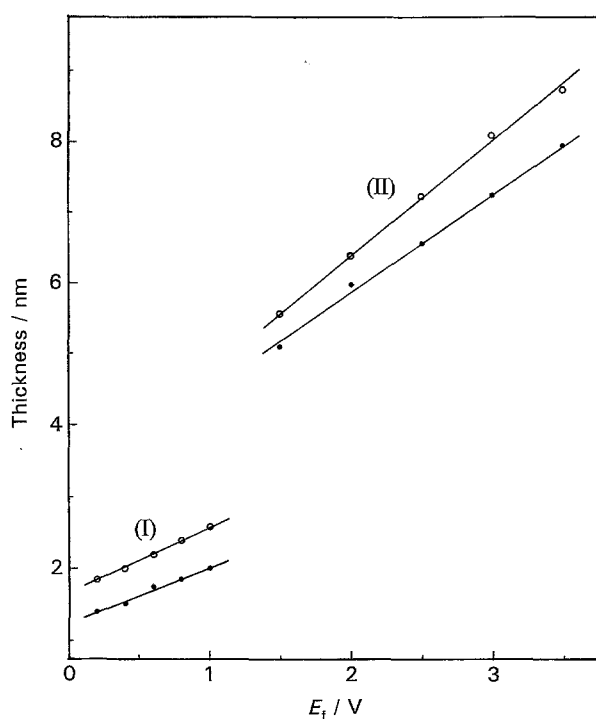


Fig. 4. Relation between the formation potential and the oxide thickness (calculated from capacitance measurements using the dielectric constant values obtained here). Oxides formed in the potential range (I) before and (II) within oxygen evolution. Key: (●) nonstabilized oxides; (○) stabilized oxides.

formation potential. Using the simple parallel plate capacitor equation, Equation 2, together with the value obtained for the dielectric constant, the oxide film thickness may be determined.

In another set of experiments, the passive films were formed potentiodynamically at  $1 \text{ mV s}^{-1}$  in the chosen background solution until the electrode potential reached the specified formation potential value. Thereafter, the film was grown further and stabilized potentiostatically at this potential for about 4 h. The thickness of these oxides was also estimated and was calculated using Equation 2. Figure 4 is a graphical representation of the relation between the calculated values of the oxide thickness and the anodic potentials used in the formation of these oxides. The following points may be observed in connection with Fig. 4: (i) that the thickness increases with increasing formation potential; (ii) that a linear relationship exists up to oxides formed at  $+1.0 \text{ V}$  (region I in Fig. 4), and that another straight line of higher slope is obtained for oxides formed from  $1.5$  to  $3.5 \text{ V}$  (region II in Fig. 4), that is, in the potential region corresponding to the oxygen evolution potential and higher potentials; (iii) that at one and the same formation potential, the stabilized oxides have higher thickness than the nonstabilized oxides; and (v) that the values of the oxide thickness formed within the potential range studied vary between  $4.0$  and  $7.95 \text{ nm}$  for nonstabilized oxides and between  $1.8$  and  $8.73 \text{ nm}$  for stabilized oxides. The oxide thicknesses for nonstabilized and stabilized oxides formed at each formation potential are given in Table 2.

To investigate the dissolution of the oxide layer in

Table 2. Thickness of the oxides (nonstabilized and stabilized) formed anodically on titanium electrodes at various formation potentials in  $\text{Na}_2\text{SO}_4 + \text{H}_2\text{SO}_4$  ( $\text{pH } 3$ ), as calculated from the capacitance measurements

$E_f / \text{V}$	Nonstabilized oxides $d/\text{nm}$	Stabilized oxides $d/\text{nm}$
0.2	1.40	1.86
0.4	1.51	2.01
0.6	1.76	2.20
0.8	1.84	2.42
1.0	2.00	2.59
1.5	5.10	5.57
2.0	6.00	6.38
2.5	6.56	7.24
3.0	7.24	8.09
3.5	7.95	8.73

the test solution, some open circuit capacitance measurements were carried out on the oxide covered titanium electrodes (nonstabilized and stabilized oxides) for about 1 h. These measurements show that the capacitance value is almost constant over an hour, indicating a constant oxide thickness. Equation 1 can be directly used to calculate oxide film thickness only with the assumption of 100% efficiency for the faradic current. Referring to Figure 1 this condition can be fulfilled only in the potential range below oxygen evolution ( $<1.5 \text{ V}$ ). In the potential range  $1.5$ – $5 \text{ V}$ , it is obvious that the current efficiency for oxide film formation must be less than unity.

Two regions can be identified in Figure 4, which represents a linear relation between the oxide film thickness (calculated with Equation 2), for both nonstabilized and stabilized oxides, with the formation potential. Region I, in the range of potential before oxygen evolution, is characterized by a relatively slow rate of oxide film formation, as indicated by the value of the anodization coefficient calculated from the slope of the thickness against formation potential relation of Figure 4. Values of anodization coefficients of  $0.77$  and  $0.91 \text{ nm V}^{-1}$  were obtained for nonstabilized and stabilized oxides, respectively. Region II in the range of potential within the oxygen evolution range is characterized by a relatively higher oxide formation rate. This is expected; oxides formed in the transpassive region tend to be thicker than those formed in the passive region [14, 15]. This can be explained by a catalytic effect of oxygen gas on the rate of oxide growth. Anodization coefficients of  $1.38$  and  $1.63 \text{ nm V}^{-1}$  for nonstabilized and stabilized oxides, respectively, were obtained in this region II.

The foregoing argument suggests that higher rates of oxide formation might be accompanied by relatively higher dielectric constant. Similar conclusions were also made earlier [6]. The higher formation rate may result in a less crystalline structure and, consequently, a lower conductivity. As the oxide thickness increases its conductivity decreases due to the decrease of concentration of donor states (oxygen

vacancies) according to the relation [16]:

$$n_d = Kd^{-2} \quad (3)$$

where  $n_d$  is the concentration of donor states and  $K$  is a constant.

### References

- [1] J. F. McAleer and L. M. Peter, *J. Electrochem Soc.* **129** (1982) 1252.
- [2] M. A. Habib, C. Bartels, J. W. Schultze and U. Stimming, *Electrochim. Acta* **27** (1982) 129.
- [3] G. Jouve, A. Politi, C. Servanti and C. Severac, *J. Microsp. Spectrosc. Electron.* **3** (1978) 513.
- [4] C. K. Dyer and J. S. L. Leach, *J. Electrochem. Soc.* **125** (1973) 1429.
- [5] R. M. Torresi, O. R. Camara and C. P. De Pauli, *Electrochim. Acta* **32** (1987) 1357.
- [6] *Idem, ibid.* **32** (1987) 1291.
- [7] W. Wilhelmsen and T. Hurlen, *ibid.* **32** (1987) 85.
- [8] F. Climent Montoliu and R. Capellades Font, *An. Quim., Ser. B* **5** (1983) 79.
- [9] M. W. Khalil, *Mat.wiss. Werkst.tech.* **23** (1992) 48.
- [10] E. M. Patrito, R. M. Torresi, E. R. M. Leiva and V. A. Macagno, *J. Electrochem. Soc.* **137** (1990) 524.
- [11] N. Baba, *J. Less-Common Metals* **43** (1972) 295.
- [12] I. A. Ammar, S. Darwish and M. W. Khalil, *Z. Werkst.tech.* **12** (1981) 421.
- [13] S. Darwish, M. W. Khalil, M. A. Abdel Rahim and I. A. Ammar, *Mat. wiss. Werkst.tech.* **20** (1989) 299.
- [14] S. Kapusta and N. Hackerman, *J. Electrochem. Soc.* **128** (1981) 327.
- [15] W. Khalil, S. Haupt and H. H. Strehblow, *Werst. Korros.* **36** (1985) 16.
- [16] K. E. Heusler and Kyung Suk Yung, *Electrochim. Acta* **22** (1977) 977.